

## Research Paper

# [6]-Gingerol induces Caspase-Dependent Apoptosis in Bladder Cancer cells via MAPK and ROS Signaling

Na Ri Choi<sup>1\*</sup>, Woo-gyun Choi<sup>1\*</sup>, Min Ji Kwon<sup>1</sup>, Joo Han Woo<sup>2,3✉</sup>, Byung Joo Kim<sup>1✉</sup>

1. Division of Longevity and Biofunctional Medicine, Pusan National University School of Korean Medicine, Yangsan 50612, Republic of Korea.
2. Department of Physiology, Dongguk University College of Medicine, Gyeongju, 38066, Republic of Korea.
3. Channelopathy Research Center (CRC), Dongguk University College of Medicine, 32 Dongguk-ro, Ilsan Dong-gu, Goyang, Gyeonggi-do, 10326, Republic of Korea.

\*These authors contributed equally to this work.

✉ Corresponding authors: **Byung Joo Kim**, Division of Longevity and Biofunctional Medicine, Pusan National University School of Korean Medicine, 49 Busandaehakro, Mulgeum-eup, Yangsan 50612, Republic of Korea. Telephone: +82-51-510-8469; Fax: +82-51-510-8420; E-mail: vision@pusan.ac.kr. **Joo Han Woo**, Department of Physiology, Dongguk University College of Medicine, Gyeongju, 38066 and Channelopathy Research Center (CRC), Dongguk University College of Medicine, 32 Dongguk-ro, Ilsan Dong-gu, Goyang, Gyeonggi-do, 10326, Republic of Korea. Telephone: +82-54-770-2418. E-mail: lsjoohan@gmail.com.

© The author(s). This is an open access article distributed under the terms of the Creative Commons Attribution License (<https://creativecommons.org/licenses/by/4.0/>). See <http://ivyspring.com/terms> for full terms and conditions.

Received: 2022.03.21; Accepted: 2022.06.09; Published: 2022.06.21

## Abstract

The anti-cancer effects of [6]-gingerol ([6]-GIN), the main active polyphenol of ginger (*Zingiber officinale*), were investigated in the human bladder cancer cell line 5637. [6]-GIN inhibited cell proliferation, increased sub-G1 phase ratios, and depolarized mitochondrial membrane potential. [6]-GIN-induced cell death was associated with the downregulation of B-cell lymphoma 2 (BCL-2) and survivin and the upregulation of Bcl-2-associated X protein (Bax). [6]-GIN activated caspase-3 and caspase-9 and regulated the activation of mitogen-activated protein kinases (MAPKs). Further, [6]-GIN also increased the intracellular reactive oxygen species (ROS) levels and TG100-115 or tranilast increased [6]-GIN-induced cell death. These results suggest that [6]-GIN induced apoptosis in the bladder cancer cell line 5637 and therefore has the potential to be used in the development of new drugs for bladder cancer treatment.

Key words: [6]-gingerol; cell proliferation; apoptosis; bladder cancer; 5637

## Introduction

Bladder cancer is one of the most frequent genitourinary malignant neoplasms [1] and non-muscle-invasive bladder cancer is the most common type of bladder cancer, accounting for 75% of the cases [2]. Currently, after surgery to remove bladder cancer, the remaining micro cancer tissues are treated with chemotherapy or radiation to prevent recurrence [3,4]. However, studies report that only a few of the current chemotherapy methods are effective in preventing the recurrence of bladder cancer [5]. Also, serious complications are known to occur [6]. Hence, more effective strategies are required for successfully treating bladder cancer.

The ginger rhizomes (*Zingiber officinale*) are among the most frequently used medicinal herbs [7]. The anti-inflammatory, anti-obesity, antiemetic, antioxidant, antibacterial, and anticancer effects of

ginger have been studied [8,9]. Ginger contains [6]-gingerol ([6]-GIN), [6]-shogaol, [6]-paradol, and zingerones [10]. Among these components, [6]-GIN (1-[49-hydroxy-39-methoxyphenyl]-5-hydroxy-3-decanone) has been known to exhibit anticancer efficacy in various cancer cell lines [11-15].

Apoptosis is the cell's natural mechanism for programmed cell death and is a promising target for anticancer therapy [16]. Hence, the prevention of cancer is one of the main functions of apoptosis [17]. However, the anti-cancer efficacy and related mechanisms of [6]-GIN in bladder cancer are not well understood. In the present study, we investigated the anticancer mechanisms of [6]-GIN in the human bladder cancer cell line 5637.

## Materials and Methods

### Reagents and cell culture

[6]-GIN was purchased from Sigma-Aldrich (St. Louis, MO, USA). Human urinary bladder carcinoma cell line 5637 was obtained from the Korean Cell Line Bank (Seoul, Korea). The cells were propagated in RPMI-1640 medium (Gibco-BRL, St. Louis, MO, USA) supplemented with 10% heat-inactivated fetal bovine serum (Invitrogen, Grand Island, NY, USA) containing 1% penicillin/streptomycin (Invitrogen), and incubated in a humidified 95% air and 5% CO<sub>2</sub> atmosphere at 37 °C.

### MTT assay

Cell viability was determined using an MTT (3-[4,5-dimethylthiazol-2-yl]-2,5-diphenyltetrazolium bromide) assay kit (Sigma-Aldrich). 5637 cells were treated with MTT solution and incubated for 2 h at 37 °C, following which, absorbance was measured at 570 nm.

### Cell cycle analysis

5637 cells were treated with ethyl alcohol and vortexed before overnight incubation at 4 °C. Samples were centrifuged for 5 min and cell pellets were resuspended in propidium iodide staining solution containing RNase (2 µL), and recentrifuged at 20000 × g for 10 s. Samples were analyzed using a fluorescence-activated cell sorter (FACScan; Becton-Dickinson, Mountain View, CA, USA) at λ = 488 nm using Cell-Quest software (Becton-Dickinson, Franklin Lakes, NJ, USA).

### Measurement of mitochondrial depolarization assay

Cells were treated with 50 nM tetramethylrhodamine methyl ester (TMRM; Sigma-Aldrich) for 30 min. Fluorescence intensities were measured using a BD FACSCANTO II (BD Biosciences, Sunnyvale, CA, USA) at the excitation and emission wavelengths of 510 and 580 nm, respectively.

### Western blot analysis

Cell lysates were prepared using RIPA buffer containing a protease and phosphatase inhibitor cocktail (Calbiochem, La Jolla, CA, USA). The total protein was quantified using Bradford assay (Bio-Rad Laboratories, Hercules, CA, USA). Equal amounts of protein (20 µg per lane) from the samples were separated by 8% or 10% SDS-PAGE and probed with the indicated antibodies. Antibodies against survivin (#2808), ERK (#9102), pERK (#9106), JNK (#9252), pJNK (#9251), p38 (#9212), and pp38 (#9216) were

purchased from Cell Signaling Technology (Danvers, MA, USA), and antibodies against Bcl (#sc-783), Bax (#sc-493), caspase-3 (#sc-7148), caspase-9 (#sc-7885), PARP (#sc-7150), β-actin (#sc-47778) and GAPDH (#sc-32233) were obtained from Santa Cruz Biotechnology (Santa Cruz, CA, USA). The secondary horseradish peroxidase-conjugated antibodies used were goat anti-rabbit IgG and goat anti-mouse IgG (SC-2004 and SC-2005, respectively; Santa Cruz Biotechnology, Dallas, TX, USA). Relative intensities of the bands were analyzed with a GS-710 Image Densitometer (Bio-Rad Laboratories). Results are representative of at least five independent experiments.

### Caspase assay

Caspase-3 and caspase-9 assay kits (Cellular Activity Assay Kit Plus; BioMol, Plymouth, PA, USA) were used. After resuspending the cells in ice-cold cell lysis buffer, the supernatant samples were incubated with a caspase substrate (400-IM Ac-DEVD-pNA; 50 µL) at 37 °C. The fluorescence of each sample was measured at 405 nm at several time-points.

### Measurement of ROS levels

Cells were treated with 20 µL DCF-DA (2',7'-dichlorodihydrofluorescein diacetate; Molecular Probes, Eugene, OR, USA) at 37 °C for 30 min and washed with PBS. Fluorescence was measured using FACS (Becton-Dickinson, Mountain View, CA, USA), at excitation and emission wavelengths of 488 and 525 nm, respectively.

### Statistical analysis

One-way ANOVA with *Dunnett's* post hoc comparison was used for multiple comparisons. The analysis was performed using Prism 6.0 (GraphPad Software Inc., La Jolla, CA, USA) and Origin 8.0 (OriginLab Corporation, Northampton, MA, USA) software. Results are expressed as means ± SEMs, and *p* values < 0.05 were considered statistically significant.

## Results

### Apoptotic effects of [6]-GIN on 5637 bladder cancer cells

The MTT assay was used after treating 5637 cells with [6]-GIN for 24 h to determine the effect of [6]-GIN on the proliferation of the cells. [6]-GIN (100, 300, or 500 µM) treatment reduced the survival of 5637 cells in a concentration and time-dependent manner (Fig. 1A). Following 24 h of treatment, the survival of 5637 cells was reduced by 84.9 ± 1.9%, 57.6 ± 0.7%, and 24.5 ± 2.2% (all *p* < 0.01) with 100, 300, and 500 µM of [6]-GIN, respectively (Fig. 1A). The survival of 5637

cells was also evaluated using the CCK method. [6]-GIN also reduced the viability of the cells by  $81.3 \pm 6.2\%$ ,  $64.9 \pm 7.4\%$ , and  $46.3 \pm 2.5\%$  (all  $p < 0.01$ ) at concentrations of 100, 300, and 500  $\mu\text{M}$ , respectively (Fig. 1B). Additionally, cell cycle analysis was conducted using flow cytometry to determine whether [6]-GIN induced apoptosis. Sub-G1 phase ratios were increased by  $6.1 \pm 1.6\%$ ,  $9.3 \pm 0.6\%$  ( $p < 0.05$ ), and  $25.7 \pm 1.8\%$  ( $p < 0.01$ ) following treatment with 100, 300, and 500  $\mu\text{M}$  [6]-GIN, respectively, when compared with the values obtained for the non-treated cells (Fig. 2A and 2B). Mitochondrial depolarization

was assessed by TMRM staining and the results showed that the mitochondrial membrane of the cells was significantly depolarized by [6]-GIN (Fig. 2C). Relative TMRM fluorescence levels were decreased by  $91.8 \pm 0.6\%$ ,  $82.4 \pm 4.4\%$  ( $p < 0.01$ ), and  $61.3 \pm 3.5\%$  ( $p < 0.001$ ) following treatment with 100, 300, and 500  $\mu\text{M}$  [6]-GIN, when compared with the values observed for the non-treated cells (Fig. 2D). These results suggested that [6]-GIN inhibited the proliferation of 5637 cells and these effects could be associated with apoptotic cell death.

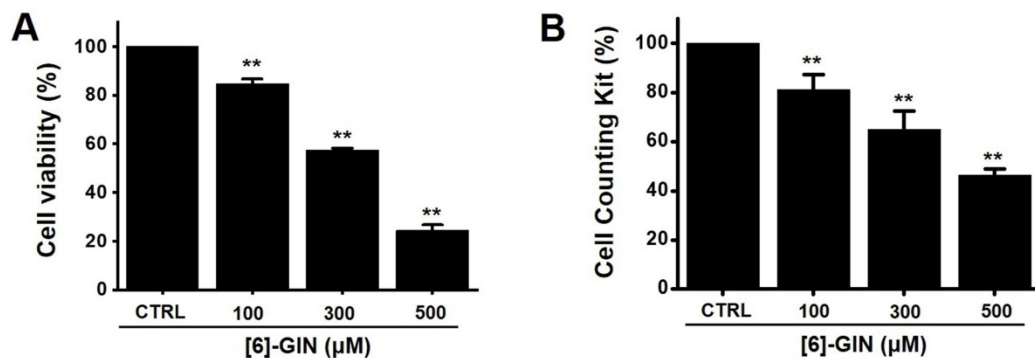


**Figure 1.** [6]-GIN reduced the cell viability of 5637 bladder cancer cells measured using MTT assay. [6]-GIN reduced cell viabilities dose-dependently after 24 h (A). (B) CCK-8 (cell counting kit-8) assays showing [6]-GIN reduced cell viability after 24 h. Bars represent mean  $\pm$  standard error. \*\* $p < 0.01$  compared with the control. [6]-GIN, [6]-gingerol. CTRL, control.

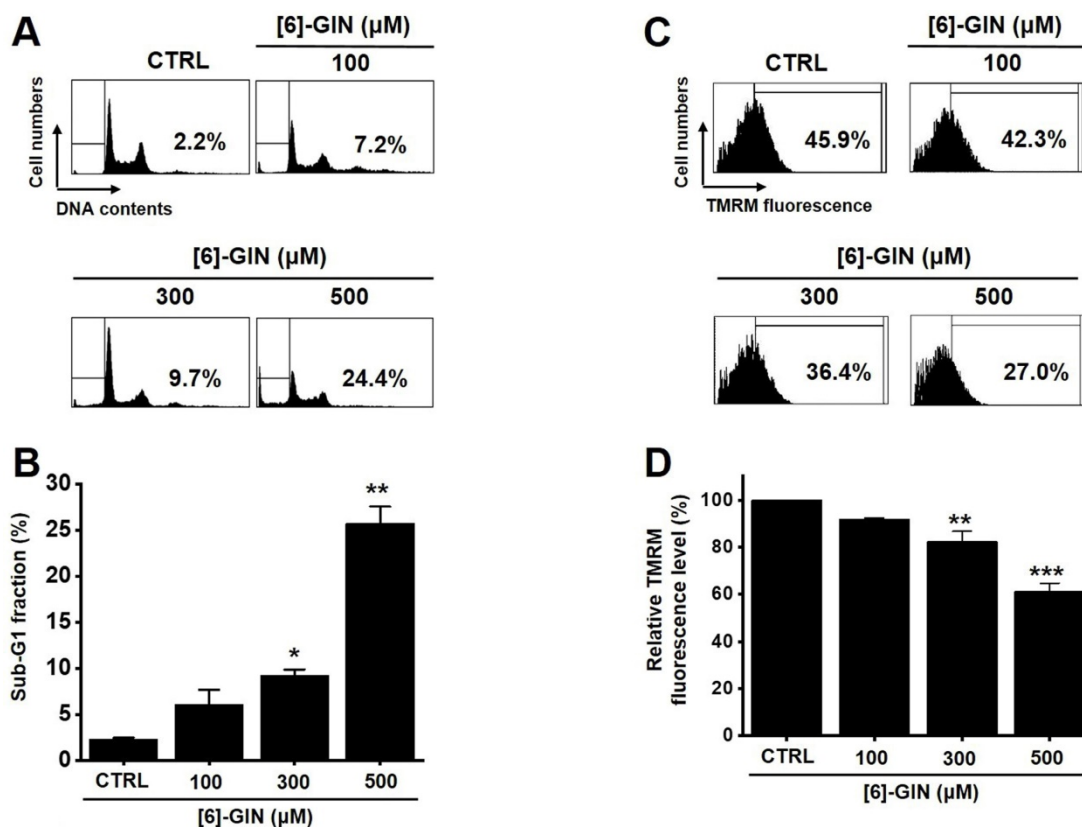


**Figure 2.** [6]-GIN increased the sub-G1 phase ratio and depolarized the mitochondrial membrane of 5637 cells. (A) Cell cycles determined with flow cytometry. (B) Sub-G1 fractions are expressed as percentages. (C) FACS analysis measured the TMRM fluorescence for mitochondrial depolarization. (D) The relative mitochondrial TMRM fluorescence levels were calculated. Bars represent mean  $\pm$  standard error. \* $p < 0.05$ . \*\* $p < 0.01$ . \*\*\* $p < 0.001$  compared with the control. [6]-GIN, [6]-gingerol. CTRL, control. TMRM, tetramethylrhodamine methyl ester.

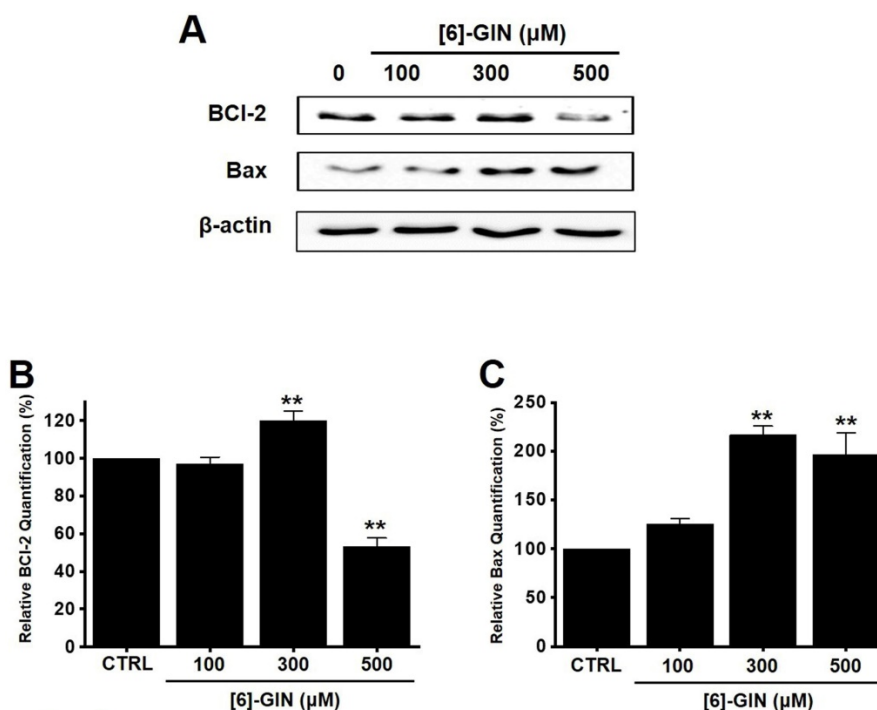


**Figure 3.** Effects of [6]-GIN on BCL-2 and Bax expression in 5637 cells determined by western blotting (A) BCL-2 expression was downregulated, whereas Bax was upregulated by [6]-GIN (B) BCL-2 and (C) Bax protein expressions were normalized versus  $\beta$ -actin. Bars represent mean  $\pm$  standard error. \*\* $p < 0.01$  compared with the control. [6]-GIN, [6]-gingerol. CTRL, control. BCL-2, B-cell lymphoma 2. Bax, BCL-2 X-associated protein.

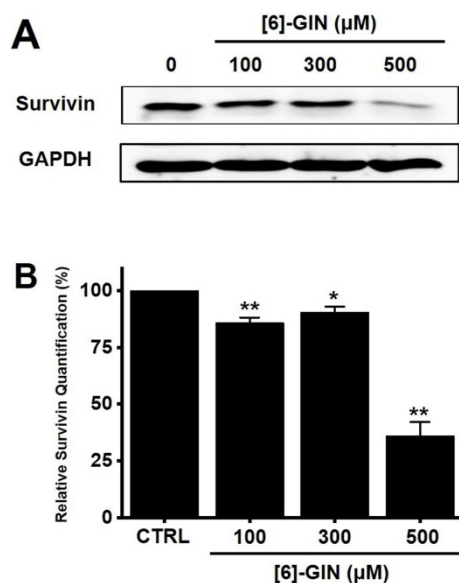


**Figure 4.** Effects of [6]-GIN on survivin expression in 5637 cells determined by western blotting. (A) Survivin expression was downregulated by [6]-GIN (B) Survivin protein expressions were normalized versus  $\beta$ -actin. Bars represent mean  $\pm$  standard error. \* $p < 0.05$ . \*\* $p < 0.01$  compared with the control. [6]-GIN, [6]-gingerol. CTRL, control.

### [6]-GIN-induced apoptosis via the mitochondrial activation mechanism

Western blotting was performed to determine whether the [6]-GIN-induced apoptosis is regulated by the BCL-2 (anti-apoptotic) and Bax (pro-apoptotic) proteins. BCL-2 levels were reduced by [6]-GIN addition, whereas the amount of Bax increased (Fig.

3A, 3B, 3C). In 5637 cells, compared with non-treated cells, relative BCL-2 levels were decreased by  $97.2 \pm 3.4\%$ ,  $119.9 \pm 5.2\%$  ( $p < 0.01$ ), and  $53.3 \pm 4.4\%$  ( $p < 0.01$ ) following treatment with 100, 300, and 500  $\mu\text{M}$  of [6]-GIN, respectively (Fig. 3B); however, the relative Bax levels were increased by  $124.9 \pm 6.2\%$ ,  $216.8 \pm 9.0\%$  ( $p < 0.01$ ), and  $196.7 \pm 22.3\%$  ( $p < 0.01$ ) upon treatment with 100, 300, and 500  $\mu\text{M}$  [6]-GIN, respectively (Fig. 3C). Expression of survivin, a member of the family of apoptosis inhibitor proteins, was also reduced by [6]-GIN (Fig. 4A, 4B). Relative survivin quantification levels were decreased by  $85.9 \pm 2.3\%$  ( $p < 0.01$ ),  $90.6 \pm 2.3\%$  ( $p < 0.05$ ), and  $36.2 \pm 5.9\%$  ( $p < 0.01$ ) at 100, 300, 500  $\mu\text{M}$  [6]-GIN, respectively, when compared with the levels observed in the non-treated cells (Fig. 4B). These results suggest that mitochondrial activation mechanisms are involved in the [6]-GIN-induced apoptosis of 5637 cells.

### [6]-GIN-induced apoptosis via caspase activation mechanism

Caspases are important mediators in apoptotic pathways. They induce the activation of cytoplasmic endonucleases, which cleave various substrates, such as poly (ADP-ribose) polymerase (PARP) as a signal for apoptosis [18]. [6]-GIN addition increased the activities of caspase-3 and caspase-9 in a dose-dependent manner, and zVAD-fmk (a broad-spectrum caspase inhibitor) suppressed these activities (Fig. 5A). Compared with the non-treated

cells, in 5637 cells, caspase-3 activity was increased by  $102.1 \pm 5.1\%$ ,  $112.1 \pm 2.1\%$ , and  $146.2 \pm 13.0\%$  ( $p < 0.01$ ) with 100, 300, and 500  $\mu\text{M}$  of [6]-GIN, respectively, and the caspase-9 activity was increased by  $111.9 \pm 3.3\%$  ( $p < 0.01$ ),  $116.5 \pm 6.4\%$  ( $p < 0.01$ ),  $124.3 \pm 0.6\%$  ( $p < 0.01$ ) with 100, 300, and 500  $\mu\text{M}$  of [6]-GIN, respectively (Fig. 5A). In addition, western blot results showed that adding [6]-GIN gradually downregulated the expression of pro-caspase-3 and pro-caspase-9 and upregulated that of active caspase-3, active caspase-9, and the PARP cleavage protein (Fig. 5B). These results suggest that caspase activation mechanisms may play a role during [6]-GIN-induced apoptosis in 5637 cells.

### [6]-GIN-induced apoptosis via mitogen-activated protein kinase (MAPK) pathways

To find out the role of MAPK pathways in [6]-GIN-induced apoptosis, cell viability was measured after [6]-GIN and PD98059 (p42/44 MAPK inhibitor) or SP600125 (c-jun NH2-terminal kinase (JNK) II inhibitor) were added together. Combination of [6]-GIN and PD98059 increased cell viability when

compared to non-treated cells (Fig. 6A), and co-administration of [6]-GIN and SP600125 increased the viability of the 5637 cells by  $90.5 \pm 2.6\%$ ,  $73.9 \pm 0.8\%$  ( $p < 0.05$ ), and  $34.1 \pm 0.6\%$  ( $p < 0.05$ ) at concentrations of 100, 300, and 500  $\mu\text{M}$ , respectively, compared with the non-treated cells (Fig. 6B). To further examine the involvement of the MAPK signaling pathways, we investigated the [6]-GIN-induced phosphorylation of MAPK proteins by western blotting. The phosphorylation of MAPKs increased after treating cells with [6]-GIN (500  $\mu\text{M}$ ) from 0.5 h to 4 h (Fig. 7A). The levels of phosphorylated extracellular signal regulated kinase (p-ERK) were increased by  $103.3 \pm 15.3\%$ ,  $173.7 \pm 29.0\%$  ( $p < 0.05$ ),  $252.3 \pm 22.0\%$  ( $p < 0.01$ ), and  $244.7 \pm 36.0\%$  ( $p < 0.01$ ) at 0.5, 1, 2, and 4 h, respectively, by [6]-GIN treatment, compared with the levels in the non-treated cells (Fig. 7B1); the p-JNK levels were also increased by  $102.1 \pm 10.0\%$ ,  $155.2 \pm 15.1\%$  ( $p < 0.05$ ),  $153.2 \pm 25.4\%$  ( $p < 0.05$ ), and  $171.2 \pm 27.1\%$  ( $p < 0.01$ ) at 0.5, 1, 2, and 4 h, respectively, by [6]-GIN treatment, compared with the levels observed in the non-treated cells (Fig. 7B2). Further, levels of p-p38 were increased

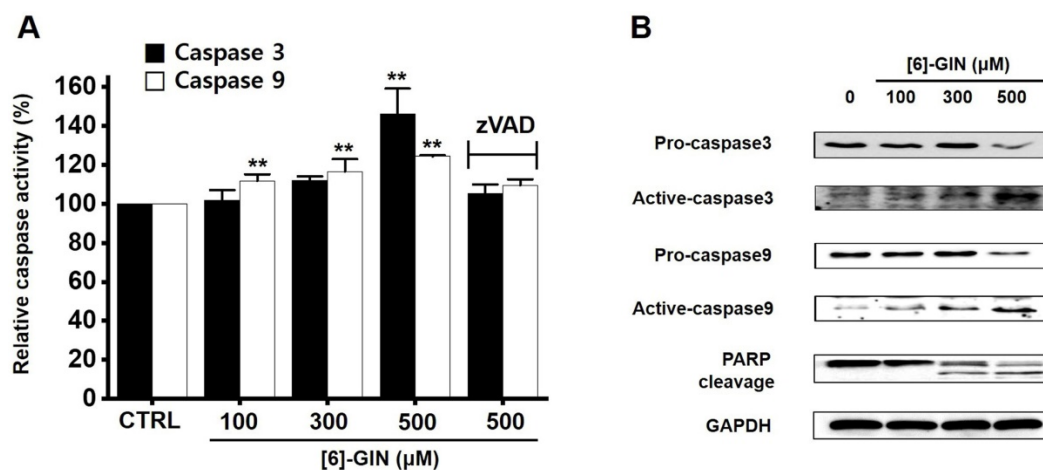


**Figure 5.** [6]-GIN-induced caspase activation in 5637 cells. **(A)** [6]-GIN increased the caspase-3 and caspase-9 activities. **(B)** Western blot analysis showed that [6]-GIN gradually down-regulated the expressions pro-caspase-3 and -9 and upregulated the active caspase-3, -9, and PARP cleavage protein levels. GAPDH was used as the internal control. Bars represent mean  $\pm$  standard error.  $**p < 0.01$  compared with the control. [6]-GIN, [6]-gingerol. CTRL, control. zVAD, carbobenzyoxy-valyl-alanyl-aspartyl-[O-methyl]- fluoromethylketone.

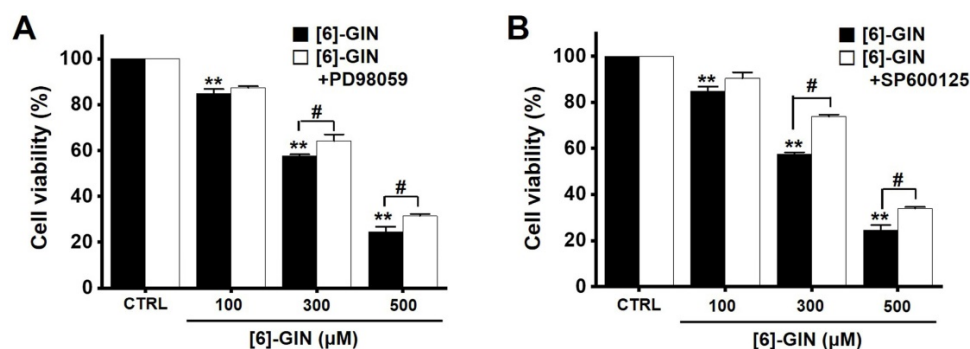


**Figure 6.** Effects of MAPK inhibitors on the activity of [6]-GIN in 5637 cells. Co-administration with [6]-GIN and **(A)** PD98059 or **(B)** SP600125 increased cell viability. Bars represent mean  $\pm$  standard error.  $**p < 0.01$  compared with the control.  $\#p < 0.05$  between treatments. [6]-GIN, [6]-gingerol. CTRL, control.

by  $238.2 \pm 23.9\%$ ,  $314.0 \pm 34.1\%$ ,  $357.1 \pm 37.0\%$ , and  $326.1 \pm 36.3\%$  (all  $p < 0.01$ ) after 0.5, 1, 2, and 4 h of [6]-GIN treatment, respectively, compared with the levels in the non-treated cells (Fig. 7B3). These results suggest that MAPK signaling pathways are likely involved in [6]-GIN-induced apoptosis.

### [6]-GIN-induced apoptosis by intracellular ROS generation

We investigated whether ROS generation was involved in [6]-GIN-induced apoptosis in 5637 cells

since ROS are reported to play an important role in apoptosis [19,20]. Flow cytometry showed that [6]-GIN significantly increased ROS production levels in 5637 cells (Fig. 8A). ROS production levels were increased by  $109.5 \pm 3.5\%$ ,  $145.0 \pm 2.8\%$  ( $p < 0.01$ ), and  $167.5 \pm 2.1\%$  ( $p < 0.01$ ) following treatment with 100, 300, and 500  $\mu\text{M}$  of [6]-GIN, respectively, compared with the levels in the non-treated cells (Fig. 8B). These results suggest that ROS generation is potentially involved in [6]-GIN-induced apoptosis.

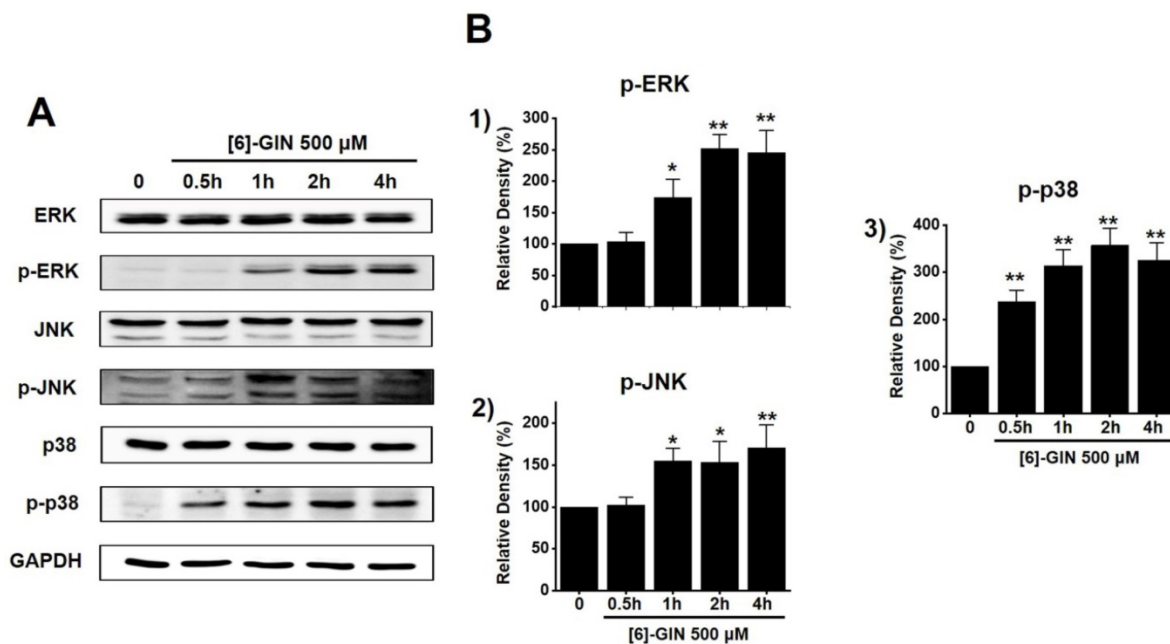


**Figure 7.** The activation of the MAPK pathways by [6]-GIN in 5637 cells. **(A)** Phosphorylation of ERK, JNK, and p38 was increased as observed by western blotting. **(B)** Phosphorylated ERK, JNK, and p38 levels are indicated as band densities relative to GAPDH. Bars represent mean  $\pm$  standard error. \* $p < 0.05$ . \*\* $p < 0.01$  compared with the control. [6]-GIN, [6]-gingerol. CTRL, control. ERK, extracellular signal-regulated kinase; JNK, c-Jun N-terminal kinase.

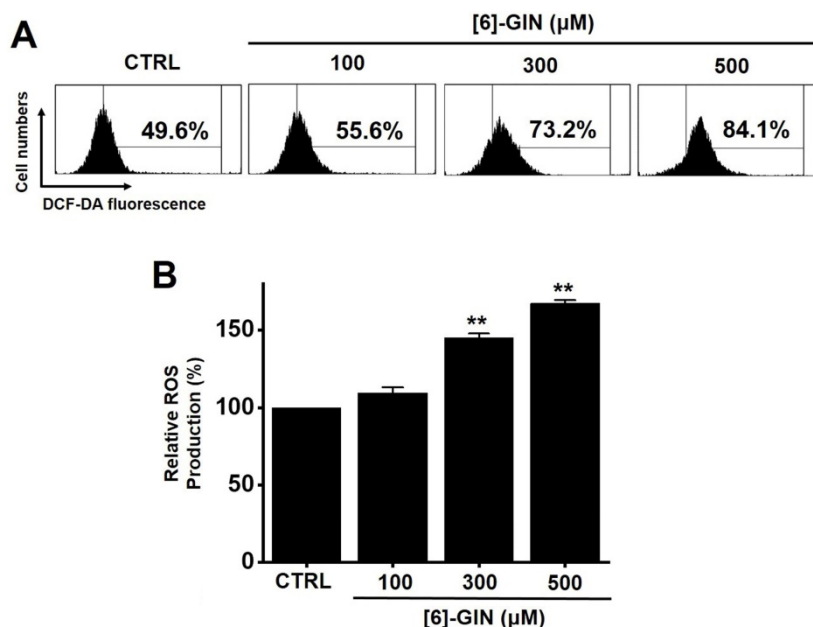


**Figure 8.** [6]-GIN increased ROS levels in 5637 cells. **(A)** Intracellular ROS levels were measured by DCF-DA. **(B)** ROS levels are expressed as percentages of untreated CTRL. Bars represent mean  $\pm$  standard error. \*\* $p < 0.01$  compared to control. [6]-GIN, [6]-gingerol. CTRL, control. ROS, reactive oxygen species. DCF-DA, 2',7'-dichlorodihydrofluorescein diacetate.

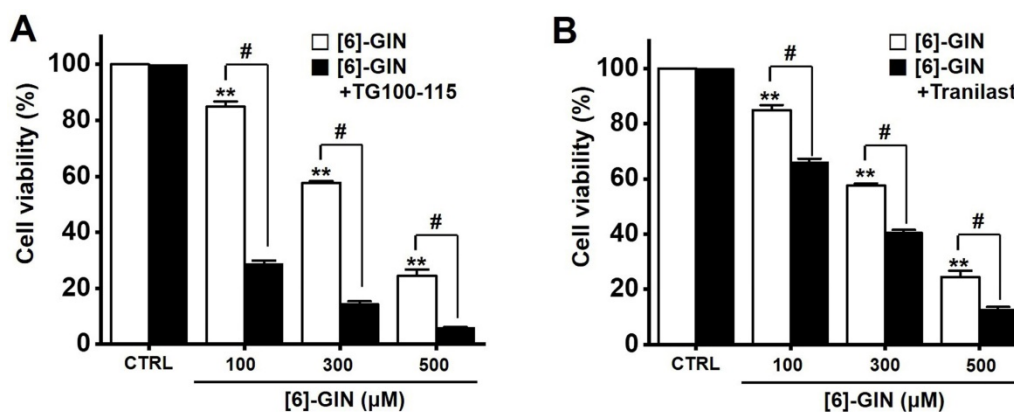


**Figure 9.** Effects of TG100-115 or tranilast on [6]-GIN-induced apoptosis in 5637 cells. Co-administration for 24 h with [6]-GIN and (A) TG100-115 or (B) Tranilast decreased the cell viability. Bars represent mean  $\pm$  standard error. \*\* $p < 0.01$  compared to control. # $p < 0.05$  between treatments. [6]-GIN, [6]-gingerol. CTRL, control.

### [6]-GIN-induced apoptosis via TRPM7 and TRPV2 ion channels

Transient receptor potential melastatin 7 (TRPM7) and vanilloid 2 (TRPV2) are nonselective cation channels that have become attractive target proteins for tumor studies due to their wide range of physiological and pathological functions [21–23]. Downregulation of TRPM7 is known to play an important role in bladder cancer cell apoptosis [21,22] and TRPV2 is known to enhance bladder cancer cell migration and invasion but not cell proliferation [23]. Therefore, we investigated whether TRPM7 and TRPV2 are involved in [6]-GIN-induced apoptosis. Cell viability was measured following co-treatment with [6]-GIN and TG100-115 (TRPM7 inhibitor) [24] or tranilast (TRPV2 inhibitor) [25]. Compared with the non-treated cells, the co-administration of [6]-GIN and TG100-115 decreased the 5637 cell viability by  $28.9 \pm 1.0\%$ ,  $14.5 \pm 0.8\%$ , and  $6.1 \pm 0.2\%$  (all  $p < 0.05$ ) at concentrations of 100, 300, and 500  $\mu\text{M}$ , respectively (Fig. 9A), and that of [6]-GIN and tranilast decreased the cell viability by  $66.2 \pm 1.1\%$ ,  $40.7 \pm 0.8\%$ , and  $12.9 \pm 0.8\%$  (all  $p < 0.05$ ) at concentrations of 100, 300, and 500  $\mu\text{M}$ , respectively (Fig. 9B). These results suggest that TRPM7 or TRPV2 cation channels are likely involved in [6]-GIN-induced apoptosis.

### Discussion

Ginger (*Zingiber officinale*) is one of the most frequently used herbs in traditional Asian medicine [7]. It contains pungent phenolic substances such as [6]-GIN, [6]-shogaol, [6]-paradol, and zingerone [10]. Among these, [6]-GIN is the main active polyphenol of ginger and has been reported to exhibit antioxidant, anti-inflammatory, anticancer, neuroprotective, anti-obesity, and anti-hepatic steatosis effects [26–32]. It is also known to have anticancer effects on various cancer cells [11–15, 33–35]. [6]-GIN has been shown to cause apoptosis in the cervical cancer cell line HeLa

by activating the caspase-3-dependent pathway [11]. In previous studies, it inhibited the metastasis of the breast cancer cell line MDA-MB-231 and caused the apoptosis of the prostate cancer cell line LNCaP [12,13]. [6]-GIN also inhibits the growth of several types of murine tumors such as melanomas, renal cell carcinomas, and colon carcinomas [14,15]. The present study demonstrates that [6]-GIN induces the apoptosis of the bladder cancer cell line 5637.

Apoptosis is a cell's natural mechanism for inducing programmed cell death and is a promising target for anticancer therapy [16]. It is caused by caspases which are a class of cysteine proteins that cleave target proteins, and this caspase protease activation is essential for apoptosis to occur [36,37]. Four initiator caspases (caspase-2, -8, -9, -10) and three executioner caspases (caspase-3, -6, -7) are known to be involved [37]. The intrinsic mechanism of apoptosis requires mitochondria and mitochondrial proteins. We conducted the MTT experiment at various time changes. In the text, cell death can be known according to the concentration at 24 hours (Fig. 1). After 48 hours or 72 hours, it was found that at 100–300  $\mu\text{M}$ , there was less death or no significant change than at 24 hours, and almost all cell death was confirmed at 500  $\mu\text{M}$ . Therefore, it can be seen that 24 hours in the text is the time to confirm the most ideal cell death in a concentration-dependent manner. The overall intrinsic pathway is regulated by the BCL-2 protein family. The anti-apoptotic BCL-2 protein inhibits apoptosis by inhibiting the proapoptotic proteins Bax and BCL-2 homologous antagonist killer [37]. In addition, the extrinsic pathway uses extracellular signals to induce apoptosis. Cell death signals bind to death receptors from the tumor necrosis factor (TNF) family [37]. In the present study, BCL-2 and survivin levels decreased, while Bax expression was increased by the addition of [6]-GIN in 5637 cells (Fig. 3 and 4). The results of [6]-GIN-induced BCL downregulation show that

[6]-GIN can cause apoptosis (Fig. 3). The change in survivin levels further supported this result (Fig. 4). Survivin is known to inhibit apoptosis and combines with the effective caspases of the apoptotic pathway, namely caspase-3 and -7 [38,39]. [6]-GIN increased the relative caspase-3 and caspase-9 activities, and their activities were suppressed by zVAD-fmk (Fig. 5). Moreover, [6]-GIN gradually downregulated pro-caspase-3 and -9 and upregulated the active caspases-3 and -9, and PARP cleavage protein expression. These results suggest that [6]-GIN induced apoptosis via caspase-dependent death receptor signaling and mitochondrial pathways. Also, we conducted experiments on autophagy. As a result of the experiment, there was no change in the expression of LC3-II. Therefore, it is thought that the autophagy process is not involved in the induction of apoptosis.

MAPKs are a family of kinases that are known to modulate gene expression, mitosis, proliferation, motility, metabolism, and apoptosis [40–44]. Particularly, they are involved in the survival and proliferation of various cancer cells, making them potential targets for cancer therapies [45]. Similarly, ROS are also essential for cell cycle regulation, differentiation, and migration [46]. ROS are important cell signaling molecules involved in the main mechanisms of apoptosis caused by mitochondria [46]. ROS are also involved in autophagy and necroptosis [46]. In this study, co-administration of [6]-GIN and PD98059 or SP600125 increased cell viability (Fig. 6) and the phosphorylation of MAPKs (Fig. 7). Furthermore, [6]-GIN increased ROS production levels (Fig. 8). These results suggest that MAPK and ROS signaling pathways are involved in the [6]-GIN-induced apoptosis mechanism.

TRP ion channels contribute to regulating various physiological and pathological responses of cells by controlling intracellular signaling and responses [47]. Among these, TRPM7 is known to be involved in important physiological processes such as intracellular  $Mg^{2+}$  regulation [48], cell viability [49], anoxic neuronal cell death [50], and gastrointestinal motility [51]. Recent studies have shown a link between TRPM7 and several cancers such as breast, ovarian, prostate, gastric, bladder, pancreatic cancers, and glioblastomas [52–57]. Other TRP ion channels called TRPV channels are critical for normal pain and temperature control [58]. TRPV2 channels have many functions, and they may be related to cancer [59,60], particularly urinary tract tumors [61,62]. TRPV2 activation induced apoptotic cell death in the T24 bladder cancer cell line [63]. In the present study, cell viability was measured after [6]-GIN and TG100-115 (TRPM7 inhibitor) or tranilast (TRPV2

inhibitor) were administered together. Co-administration of [6]-GIN and TG100-115 or tranilast decreased the cell viability (Fig. 9). These results suggest that TRPM7 or TRPV2 cation channels are involved in [6]-GIN-induced apoptosis. However, a potent and dual selective phosphoinositide 3-kinase (PI3K) inhibitor is well known in TG100-115 [64] and is also found to be effective as a TRPM7 inhibitor [24]. Tranilast is known for its efficacy in antiallergic function and inhibitor of angiogenesis [65,66] and its function as a TRPV2 inhibitor has also been revealed [25]. There are always various effects when researching using inhibitors, so be careful when you think about the results. Therefore, we think that more in-depth research is needed such as using various inhibitors to compare results with each other. TG100-115 also has the function of PI3K $\gamma/\delta$  inhibitor [67]. Therefore, we checked the relevance of this function. We used GDC-0032 with the function of PI3K $\gamma/\delta$  inhibitor [68]. As a result of the experiment, some apoptosis was observed in the presence of GDC-0032, but no apoptosis to the extent of TG100-115. Therefore, the reaction by TG100-115 is considered to be the result obtained by inhibiting TRPM7 rather than the reaction by PI3K $\gamma/\delta$  inhibition. Several TRP ion channels are associated with cancer apoptosis and are potential therapeutic targets [69]. The most representative TRP ion channel is TRPM8. TRPM8 is overexpressed in prostate cancer and its expression level is associated with cancer cell death [70]. At the same time, menthol, a TRPM8 activator, inhibits the proliferation of prostate cancer cell lines. Because patients with chronic prostatic hyperplasia often develop prostate cancer, they may benefit from TRPM8 activator therapy [71]. Therefore, in this study, the relevance of TRPM7 or TRPV2 was mentioned. In the future, the possibility of other ion channels such as TRPM8 will be further studied.

In conclusion, the present study shows that [6]-GIN inhibits cell proliferation, increases sub-G1 phase ratios, and depolarizes mitochondrial membrane potential in 5637 bladder cancer cells. [6]-GIN-induced apoptosis of cancer cells was associated with proteins such as BCL-2, survivin, Bax, caspase-3 and caspase-9, and MAPK. Intracellular ROS levels regulate the [6]-GIN-induced cell death and TG100-115 or tranilast had an effect of enhancing the [6]-GIN-induced cell death. We believe that the results of this study could serve as a basis for the future development of new drugs for bladder cancer treatment.

## Acknowledgements

This study was supported by Basic Science Research Program through the National Research

Foundation of Korea (NRF) funded by the Ministry of Education (2021R111A3042479) and the Dongguk University Research Program of 2021.

## Competing Interests

The authors have declared that no competing interest exists.

## References

- Siegel RL, Miller KD, Jemal A. Cancer statistics, 2020. *CA Cancer J Clin.* 2020; 70: 7–30.
- Grayson M. Bladder cancer. *Nature.* 2017; 551: 533.
- Zhu YT, Pang SY, Lei CY, et al. Development of a therapy against metastatic bladder cancer using an interleukin-2 surface-modified MB49 bladder cancer stem cells vaccine. *Stem Cell Res Ther.* 2015; 6: 224.
- Yin M, Joshi M, Meijer RP, et al. Neoadjuvant chemotherapy for muscle-invasive bladder cancer: a systematic review and two-step meta-analysis. *Oncologist.* 2016; 21: 708–15.
- Boegemann M, Aydin AM, Bagrodia A, et al. Prospects and progress of immunotherapy for bladder cancer. *Expert Opin Biol Ther.* 2017; 17: 1417–31.
- Veeratterapillay R, Heer R, Johnson MI, et al. High-risk non-muscle-invasive bladder cancer therapy options during intravesical BCG shortage. *Curr Urol Rep.* 2016; 17: 68.
- Gawel K, Kukula-Koch W, Banono NS, et al. 6-Gingerol, a Major Constituent of *Zingiber officinale* Rhizoma, Exerts Anticonvulsant Activity in the Pentylentetrazole-Induced Seizure Model in Larval Zebrafish. *Int J Mol Sci.* 2021; 22: 7745.
- Baliga MS, Haniadka R, Pereira MM, et al. Update on the chemopreventive effects of ginger and its phytochemicals. *Crit Rev Food Sci Nutr.* 2011; 51: 499–523.
- Shukla Y, Singh M. Cancer preventive properties of ginger: a brief review. *Food Chem Toxicol.* 2007; 45: 683–90.
- Surh YJ, Lee E, Lee JM. Chemoprotective properties of some pungent ingredients present in red pepper and ginger. *Mutat Res.* 1998; 402: 259–67.
- Chakraborty D, Bishayee K, Ghosh S, et al. [6]-Gingerol induces caspase 3 dependent apoptosis and autophagy in cancer cells: drug-DNA interaction and expression of certain signal genes in HeLa cells. *Eur J Pharmacol.* 2012; 694: 20–9.
- Lee HS, Seo EY, Kang NE, et al. [6]-Gingerol inhibits metastasis of MDA-MB-231 human breast cancer cells. *J Nutr Biochem.* 2008; 19: 313–9.
- Shukla Y, Prasad S, Tripathi C, et al. *In vitro* and *in vivo* modulation of testosterone mediated alterations in apoptosis related proteins by [6]-gingerol. *Mol Nutr Food Res.* 2007; 51: 1492–502.
- Ju SA, Park SM, Lee YS, et al. Administration of 6-gingerol greatly enhances the number of tumor-infiltrating lymphocytes in murine tumors. *Int J Cancer.* 2012; 130: 2618–28.
- Park KK, Chun KS, Lee JM, et al. Inhibitory effects of [6]-gingerol, a major pungent principle of ginger, on phorbol ester-induced inflammation, epidermal ornithine decarboxylase activity and skin tumor promotion in ICR mice. *Cancer Lett.* 1998; 129: 139–44.
- Pfeffer CM, Singh ATK. Apoptosis: A Target for Anticancer Therapy. *Int J Mol Sci.* 2018; 19: 448.
- Lopez J, Tait SWG. Mitochondrial apoptosis: Killing cancer using the enemy within. *Br J Cancer.* 2015; 112: 957–62.
- Boulares AH, Zoltoski AJ, Contreras FJ, et al. Regulation of DNAS1L3 endonuclease activity by poly(ADP-ribosylation) during etoposide-induced apoptosis. Role of poly(ADP-ribose) polymerase-1 cleavage in endonuclease activation. *J Biol Chem.* 2002; 277: 372–8.
- Matés JM, Sánchez-Jiménez FM. Role of reactive oxygen species in apoptosis: implications for cancer therapy. *Int J Biochem Cell Biol.* 2000; 32: 157–70.
- Redza-Dutordoir M, Averill-Bates DA. Activation of apoptosis signalling pathways by reactive oxygen species. *Biochim Biophys Acta.* 2016; 1863: 2977–92.
- Gao SL, Kong CZ, Zhang Z, et al. TRPM7 is overexpressed in bladder cancer and promotes proliferation, migration, invasion and tumor growth. *Oncol Rep.* 2017; 38: 1967–76.
- Cao R, Meng Z, Liu T, et al. Decreased TRPM7 inhibits activities and induces apoptosis of bladder cancer cells via ERK1/2 pathway. *Oncotarget.* 2016; 7: 72941–60.
- Liu Q, Wang X. Effect of TRPV2 cation channels on the proliferation, migration and invasion of 5637 bladder cancer cells. *Exp Ther Med.* 2013; 6: 1277–82.
- Song C, Bae Y, JinJoo Jun JJ, et al. Identification of TG100-115 as a new and potent TRPM7 kinase inhibitor, which suppresses breast cancer cell migration and invasion. *Biochim Biophys Acta Gen Subj.* 2017; 1861: 947–57.
- Iwata Y, Katayama Y, Okuno Y, et al. Novel inhibitor candidates of TRPV2 prevent damage of dystrophic myocytes and ameliorate against dilated cardiomyopathy in a hamster model. *Oncotarget.* 2018; 9: 14042–57.
- Dugasani S, Pichika MR, Nadarajah VD, et al. Comparative antioxidant and anti-inflammatory effects of [6]-gingerol, [8]-gingerol, [10]-gingerol and [6]-shogaol. *J Ethnopharmacol.* 2010; 127: 515–20.
- Abolaji AO, Ojo M, Afolabi TT, et al. Protective properties of 6-gingerol-rich fraction from *Zingiber officinale* (Ginger) on chlorpyrifos-induced oxidative damage and inflammation in the brain, ovary and uterus of rats. *Chem Biol Interact.* 2017; 270: 15–23.
- Poltronieri J, Becceneri AB, Fuzer AM, et al. [6]-gingerol as a cancer chemopreventive agent: a review of its activity on different steps of the metastatic process. *Mini Rev Med Chem.* 2014; 14: 313–21.
- Zhang F, Zhang JG, Yang W, et al. 6-Gingerol attenuates LPS-induced neuroinflammation and cognitive impairment partially via suppressing astrocyte overactivation. *Biomed Pharmacother.* 2018; 107: 1523–9.
- Liu L, Yao L, Wang S, et al. 6-Gingerol improves ectopic lipid accumulation, mitochondrial dysfunction, and insulin resistance in skeletal muscle of ageing rats: dual stimulation of the AMPK/PGC-1α signaling pathway via plasma adiponectin and muscular AdipoR1. *Mol Nutr Food Res.* 2019; 63: e1800649.
- Li J, Wang S, Yao L, et al. 6-gingerol ameliorates age-related hepatic steatosis: association with regulating lipogenesis, fatty acid oxidation, oxidative stress and mitochondrial dysfunction. *Toxicol Appl Pharmacol.* 2019; 362: 125–35.
- Tzeng TF, Liou SS, Chang CJ, et al. [6]-gingerol dampens hepatic steatosis and inflammation in experimental nonalcoholic steatohepatitis. *Phytomedicine.* 2015; 22: 452–61.
- Jeong CH, Bode AM, Pugliese A, et al. [6]-Gingerol suppresses colon cancer growth by targeting leukotriene A4 hydrolase. *Cancer Res.* 2009; 69: 5584–91.
- Lin CB, Lin CC, Tsay GJ. 6-Gingerol Inhibits Growth of Colon Cancer Cell LoVo via Induction of G2/M Arrest. *Evid Based Complement Alternat Med.* 2012; 2012: 326096.
- Radhakrishnan EK, Bava SV, Narayanan SS, et al. [6]-Gingerol induces caspase-dependent apoptosis and prevents PMA-induced proliferation in colon cancer cells by inhibiting MAPK/AP-1 signaling. *PLoS One.* 2014; 9: e104401.
- Lopez J, Tait SWG. Mitochondrial apoptosis: Killing cancer using the enemy within. *Br J Cancer.* 2015; 112: 957–62.
- Zaman S, Wang R, Gandhi V. Targeting the apoptosis pathway in hematologic malignancies. *Leuk Lymphoma.* 2014; 55: 1980–92.
- Mobahat M, Narendran A, Riabowol K, et al. Survivin as a preferential target for cancer therapy. *Int J Mol Sci.* 2014; 15: 2494–516.
- Chen X, Duan N, Zhang C, et al. Survivin and tumorigenesis: molecular mechanisms and therapeutic strategies. *J Cancer.* 2016; 7: 314–23.
- Johnson GL and Lapadat R. Mitogen-activated protein kinase pathways mediated by ERK, JNK, and p38 protein kinases. *Science.* 2002; 298: 1911–12.
- Werlen G, Hausmann B, Naeher D, et al. Signaling life and death in the thymus: timing is everything. *Science.* 2003; 299: 1859–63.
- Gupta J, Igea A, Papaioannou M, et al. Pharmacological inhibition of p38 MAPK reduces tumor growth in patient-derived xenografts from colon tumors. *Oncotarget.* 2015; 6: 8539–51.
- Miguel JC, Maxwell AA, Hsieh JJ, et al. Epidermal growth factor suppresses intestinal epithelial cell shedding via a MAPK dependent pathway. *J Cell Sci.* 2017; 130: 90–6.
- Ge X, Liu J, Shi Z, et al. Inhibition of MAPK signaling pathways enhances cell death induced by 5-Aminolevulinic acid-photodynamic therapy in skin squamous carcinoma cells. *Eur J Dermatol.* 2016; 26: 164–72.
- Wada T, Penninger JM. Mitogen-activated protein kinases in apoptosis regulation. *Oncogene.* 2004; 23: 2838–49.
- Redza-Dutordoir M, Averill-Bates DA. Activation of apoptosis signalling pathways by reactive oxygen species. *Biochim Biophys Acta.* 2016; 1863: 2977–92.
- Clapham DE. TRP channels as cellular sensors. *Nature.* 2003; 426: 517–24.
- Paravicini TM, Chubanov V, Gudermann T. TRPM7: a unique channel involved in magnesium homeostasis. *Int J Biochem Cell Biol.* 2012; 44: 1381–4.
- Nadler MJ, Hermosura MC, Inabe K, et al. LTRPC7 is a Mg<sup>2+</sup>-ATP-regulated divalent cation channel required for cell viability. *Nature.* 2001; 411: 590–5.
- Aarts M, Ihara K, Wei WL, et al. A key role for TRPM7 channels in anoxic neuronal death. *Cell.* 2003; 115: 863–77.
- Kim BJ, Lim HH, Yang DK, et al. Melastatin-type transient receptor potential channel 7 is required for intestinal pacemaker activity. *Gastroenterology.* 2005; 129: 1504–17.
- Kim BJ, Park EJ, Lee JH, et al. Suppression of transient receptor potential melastatin 7 channel induces cell death in gastric cancer. *Cancer Sci.* 2008; 99: 2502–9.
- Guilbert A, Gautier M, Dhennin-Duthille I, et al. Transient receptor potential melastatin 7 is involved in oestrogen receptor-negative metastatic breast cancer cells migration through its kinase domain. *Eur J Cancer.* 2013; 49: 3694–707.
- Wang J, Liao QJ, Zhang Y, et al. TRPM7 is required for ovarian cancer cell growth, migration and invasion. *Biochem Biophys Res Commun.* 2014; 454: 547–53.
- Lin CM, Ma JM, Zhang L, et al. Inhibition of transient receptor potential melastatin 7 enhances apoptosis induced by TRAIL in PC-3 cells. *Asian Pac J Cancer Prev.* 2015; 16: 4469–75.
- Chen WL, Barszczyk A, Turlova E, et al. Inhibition of TRPM7 by carvacrol suppresses glioblastoma cell proliferation, migration and invasion. *Oncotarget.* 2015; 6: 16321–40.

57. Yee NS, Kazi AA, Li Q, et al. Aberrant over-expression of TRPM7 ion channels in pancreatic cancer: Required for cancer cell invasion and implicated in tumor growth and metastasis. *Biol Open*. 2015; 4: 507-14.
58. Liu Q, Wang X. Effect of TRPV2 cation channels on the proliferation, migration and invasion of 5637 bladder cancer cells. *Exp Ther Med*. 2013; 6: 1277-82.
59. Prevarskaya N, Zhang L, Barritt G. TRP channels in cancer. *Biochim Biophys Acta*. 2007; 1772: 937-46.
60. Santoni G, Farfariello V. TRP channels and cancer: new targets for diagnosis and chemotherapy. *Endocr Metab Immune. Disord Drug Targets*. 2011; 11: 54-67.
61. Prevarskaya N, Flourakis M, Bidaux G, et al. Differential role of TRP channels in prostate cancer. *Biochem Soc Trans*. 2007; 35: 133-5.
62. Ziglioli F, Frattini A, Maestroni U, et al. Vanilloid-mediated apoptosis in prostate cancer cells through a TRPV-1 dependent and a TRPV-1-independent mechanism. *Acta Biomed*. 2009; 80: 13-20.
63. Yamada T, Ueda T, Shibata Y, et al. TRPV2 activation induces apoptotic cell death in human T24 bladder cancer cells: a potential therapeutic target for bladder cancer. *Urology*. 2010; 76: 509.e1-7.
64. Lee YS, Song SJ, Hong HK, et al. The FBW7-MCL-1 axis is key in M1 and M2 macrophage-related colon cancer cell progression: validating the immunotherapeutic value of targeting PI3Ky. *Exp Mol Med*. 2020; 52: 815-31.
65. Jin D, Takai S, Shiota N, et al. Tranilast, an anti-allergic drug, possesses antagonistic potency to angiotensin II. *Eur J Pharmacol*. 1998; 361: 199-205.
66. Connors CR, Rosenman DJ, Lopes DHJ, et al. Tranilast binds to A $\beta$  monomers and promotes A $\beta$  fibrillation. *Biochemistry*. 2013; 52: 3995-4002.
67. John Doukas J, Wrasidlo W, Noronha G, et al. Phosphoinositide 3-kinase gamma/delta inhibition limits infarct size after myocardial ischemia/reperfusion injury. *Proc Natl Acad Sci U S A*. 2006; 103: 19866-71.
68. Lee M, Song Y, Choi I, et al. Expression of HYOU1 via Reciprocal Crosstalk between NSCLC Cells and HUVECs Control Cancer Progression and Chemoresistance in Tumor Spheroids. *Mol Cells*. 2021; 44: 50-62.
69. Prevarskaya N, Zhang L, Barritt G. TRP channels in cancer. *Biochim Biophys Acta*. 2007; 1772: 937-46.
70. Zhang L, Barritt GJ. TRPM8 in prostate cancer cells: a potential diagnostic and prognostic marker with a secretory function? *Endocr Relat Cancer*. 2006; 13: 27-38.
71. Grolez GP, Gkika D. TRPM8 Puts the Chill on Prostate Cancer. *Pharmaceuticals (Basel)*. 2016; 9(3): 44.